

The environment of pulsar halo progenitors

Lioni-Moana Bourguinat
Carmelo Evoli, Pierrick Martin, Sarah Recchia

TeV Halos

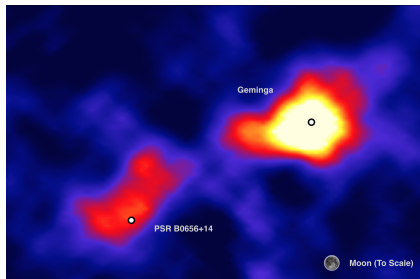


Figure: HAWC sky map of TeV emission from Geminga and its neighbour PSR B0656+14.
Credits: HAWC Collaboration

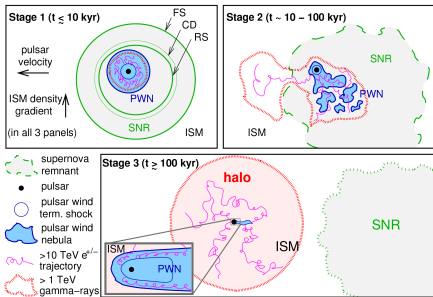


Figure: Sketch of the main evolutionary stages of a pulsar wind nebula.
Credits: Giacinti et al. (2020)

TeV Halos

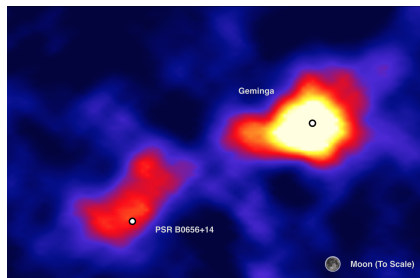


Figure: HAWC sky map of TeV emission from Geminga and its neighbour PSR B0656+14.
Credits: HAWC Collaboration

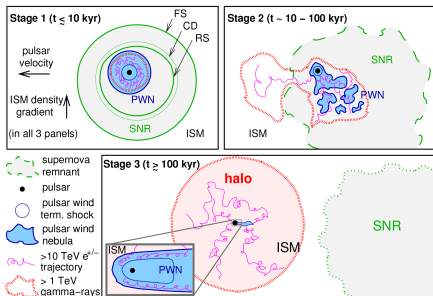


Figure: Sketch of the main evolutionary stages of a pulsar wind nebula.
Credits: Giacinti et al. (2020)

Standard assumption

Pulsar **outside** the SNR \rightarrow Low diffusion coefficient problem [Abeysekera et al. (2017)]

Solving the diffusion coefficient problem

Theoretical explanations

- Cosmic-ray induced turbulence [Evoli, Linden, et al. (2018), Mukhopadhyay et al. (2022)]
- **Environment induced turbulence** [Fang et al. (2019), Schroer et al. (2022)]

Theoretical explanations

- Cosmic-ray induced turbulence [Evoli, Linden, et al. (2018), Mukhopadhyay et al. (2022)]
- **Environment induced turbulence** [Fang et al. (2019), Schroer et al. (2022)]

Which medium are the leptons probing when we see a TeV halo?

Theoretical explanations

- Cosmic-ray induced turbulence [Evoli, Linden, et al. (2018), Mukhopadhyay et al. (2022)]
- **Environment induced turbulence** [Fang et al. (2019), Schroer et al. (2022)]

Which medium are the leptons probing when we see a TeV halo?

Where is the pulsar at a given age?

Method

Computation of the escape time from the SNR of a population of pulsars using a Monte Carlo approach for 3 models:

- ISM (interstellar medium)
- CSM (circumstellar medium)
- SB (superbubble)

Property of the pulsars: Kick velocity

Kick velocity distribution

Taken from [Faucher-Giguère et al. \(2006\)](#), modulus of all components:

$$f(v_k^{x,y,z}) = w \mathcal{N}(v_k, \sigma = 160 \text{ km/s}) + (1 - w) \mathcal{N}(v_k, \sigma = 780 \text{ km/s}) \quad (1)$$

with $w = 0.90$.

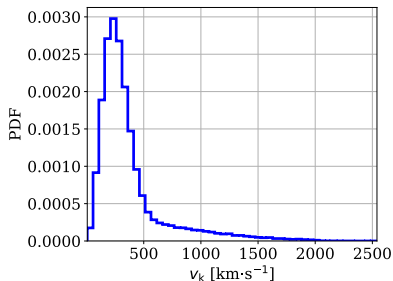


Figure: PDF of the kick velocity of pulsars.

Assumptions

- **Constant interstellar medium** around the CC SN
- Distributions of E_{SN} and n_{ISM}

Assumptions

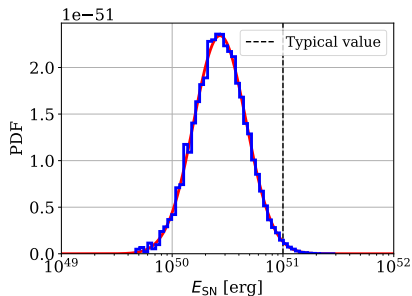
- **Constant interstellar medium** around the CC SN
- Distributions of E_{SN} and n_{ISM}

SNR evolution

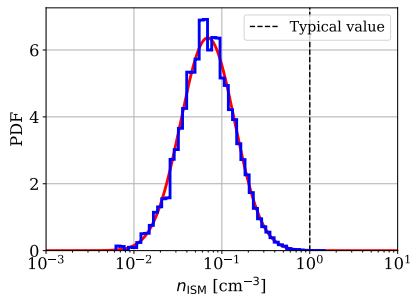
Analytical solutions following [Cioffi et al. \(1988\)](#), compared with the calculator by [Leahy and Williams \(2017\)](#):

- Sedov-Taylor phase
- Pressure-Driven Snowplough phase
- (Momentum Conserving Stage)
- Merger with the ISM

ISM model: SN energy and ISM density



(a) Effective E_{SN} PDF, $\mu = 2.7 \times 10^{50}$ erg, $\sigma = 3.5$



(b) Effective n_{ISM} PDF, $\mu = 0.069$ cm^{-3} , $\sigma = 5.1$

Figure: Lognormal distributions, following [Leahy, Ranasinghe, et al. \(2020\)](#). Computed by assuming a constant ISM density surrounding each of 43 SNe.

ISM model: Escape time

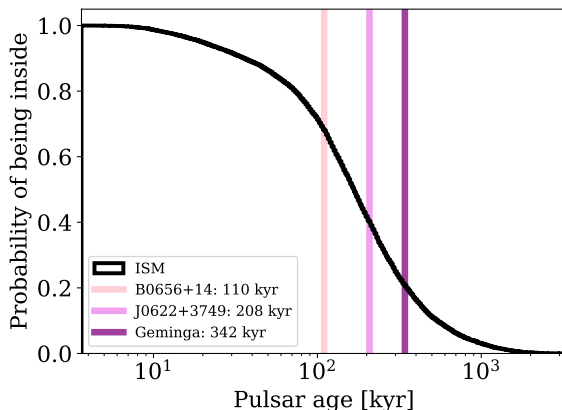


Figure: Probability of pulsars being inside the **SNR** as a function of time for the **ISM** model. Characteristic ages of pulsars are orders of magnitude, taken from the catalog of [Manchester et al. \(2005\)](#).

Assumptions

- CC SN happens in the **circumstellar medium** shaped by the progenitor

Assumptions

- CC SN happens in the **circumstellar medium** shaped by the progenitor

Process

- Pick a random **progenitor mass** from a Galactic Initial Mass Function (IMF),
- **Star properties** [Seo et al. (2018)],
- **Bubble properties** [Weaver et al. (1977), Härer et al. (2023)].

Neglecting post-MS phases for the wind and bubble structure.

Assumptions

- CC SN happens in the **circumstellar medium** shaped by the progenitor

Process

- Pick a random **progenitor mass** from a Galactic Initial Mass Function (IMF),
- **Star properties** [Seo et al. (2018)],
- **Bubble properties** [Weaver et al. (1977), Härer et al. (2023)].

Neglecting post-MS phases for the wind and bubble structure.

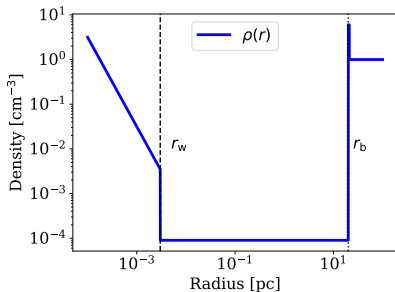


Figure: Density profile in the CSM, based on Weaver et al. (1977).

CSM model: Comparing the shell mass and the SNR mass

Parameters for a star of

$$M_{\text{ZAMS}} = 8 M_{\odot}$$

- Bubble radius $r_b = 20 \text{ pc}$,
- Surrounding ISM density of $n_{\text{ISM}} = 1 \text{ cm}^{-3}$,
- Mass lost in winds
 $\Delta M_{\text{MS}} = 0.1 M_{\odot}$ and
 $\Delta M_{\text{RSG}} = 3.4 M_{\odot}$,
- Ejecta mass is
 $M_{\text{ZAMS}} - \Delta M_{\text{MS}} - \Delta M_{\text{RSG}} -$
 $M_{\text{pulsar}} = M_{\text{ej}} = 3.1 M_{\odot}$,
- Mass swept in the bubble by the SNR is the mass lost in winds.

CSM model: Comparing the shell mass and the SNR mass

Parameters for a star of

$$M_{\text{ZAMS}} = 8 M_{\odot}$$

- Bubble radius $r_b = 20 \text{ pc}$,
- Surrounding ISM density of $n_{\text{ISM}} = 1 \text{ cm}^{-3}$,
- Mass lost in winds $\Delta M_{\text{MS}} = 0.1 M_{\odot}$ and $\Delta M_{\text{RSG}} = 3.4 M_{\odot}$,
- Ejecta mass is $M_{\text{ZAMS}} - \Delta M_{\text{MS}} - \Delta M_{\text{RSG}} - M_{\text{pulsar}} = M_{\text{ej}} = 3.1 M_{\odot}$,
- Mass swept in the bubble by the SNR is the mass lost in winds.

Computations

$$M_{\text{shell}} = \frac{4\pi}{3} \rho_{\text{ISM}} r_b^3 = 755 M_{\odot} \quad (2)$$

Mass ratio:

$$\frac{M_{\text{shell}}}{M_{\text{ej}} + \Delta M} = 116 \quad (3)$$

Shell stops the expansion of the SNR

CSM model: Comparing the shell mass and the SNR mass

Parameters for a star of

$$M_{\text{ZAMS}} = 8 M_{\odot}$$

- Bubble radius $r_b = 20 \text{ pc}$,
- Surrounding ISM density of $n_{\text{ISM}} = 1 \text{ cm}^{-3}$,
- Mass lost in winds $\Delta M_{\text{MS}} = 0.1 M_{\odot}$ and $\Delta M_{\text{RSG}} = 3.4 M_{\odot}$,
- Ejecta mass is $M_{\text{ZAMS}} - \Delta M_{\text{MS}} - \Delta M_{\text{RSG}} - M_{\text{pulsar}} = M_{\text{ej}} = 3.1 M_{\odot}$,
- Mass swept in the bubble by the SNR is the mass lost in winds.

Computations

$$M_{\text{shell}} = \frac{4\pi}{3} \rho_{\text{ISM}} r_b^3 = 755 M_{\odot} \quad (2)$$

Mass ratio:

$$\frac{M_{\text{shell}}}{M_{\text{ej}} + \Delta M} = 116 \quad (3)$$

Shell stops the expansion of the SNR

Conclusion

Boundary: bubble radius instead of the SNR

Assumptions

- Point-like cluster surrounded by a **superbubble** [Weaver et al. (1977)]
- Ambient density of $n_{\text{ISM}} \sim 100 \text{ cm}^{-3}$ [Parizot et al. (2004)]
- The SNR is very fast or merges within the SB [Mac Low et al. (1988)]

Assumptions

- Point-like cluster surrounded by a **superbubble** [Weaver et al. (1977)]
- Ambient density of $n_{\text{ISM}} \sim 100 \text{ cm}^{-3}$ [Parizot et al. (2004)]
- The SNR is very fast or merges within the SB [Mac Low et al. (1988)]

Process

Pick a **random cluster mass** following a cluster IMF [Portegies Zwart et al. (2010)].

Populate with stars following the Galactic IMF.

Compute the **cluster luminosity** and SB radius [Weaver et al. (1977), Härer et al. (2023)].

Pick a **random massive star** and find the associated MS time [Seo et al. (2018)].

Creation of a pulsar at the MS time and propagation of both pulsar and SB radius.

Comparing the probability of being inside the boundary

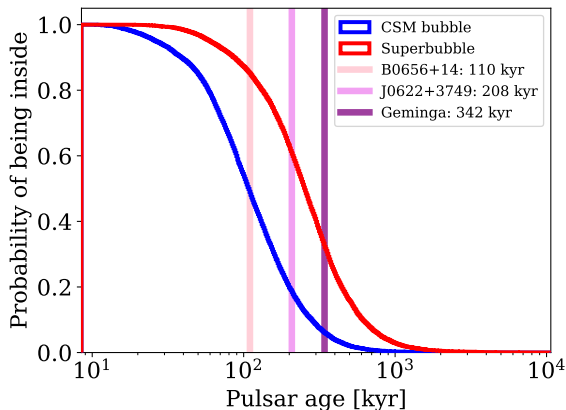


Figure: Probability of pulsars being inside the **bubble (SB)** as a function of time for the **CSM (SB) models** respectively.

Some numbers

Pulsar	Age [kyr]	Inside (CSM, 4% ¹)	Inside (SB, 96% ¹)
B0656+14	110	49%	85%
J0622+3749	208	19%	61%
Geminga	342	6%	33%

¹of O stars[de Wit et al. (2005)]

Some numbers

Pulsar	Age [kyr]	Inside (CSM, 4% ¹)	Inside (SB, 96% ¹)
B0656+14	110	49%	85%
J0622+3749	208	19%	61%
Geminga	342	6%	33%

More on Geminga

Hints that Geminga is in a hot ionized medium:

- No H_{α} lines in the near vicinity [Caraveo et al. (2003)]
- Proximity to Gemini H_{α} Ring bubble [Knies et al. (2018)]

¹of O stars[de Wit et al. (2005)]

Comparing the probability of being inside the boundary

Changing the maximum star mass

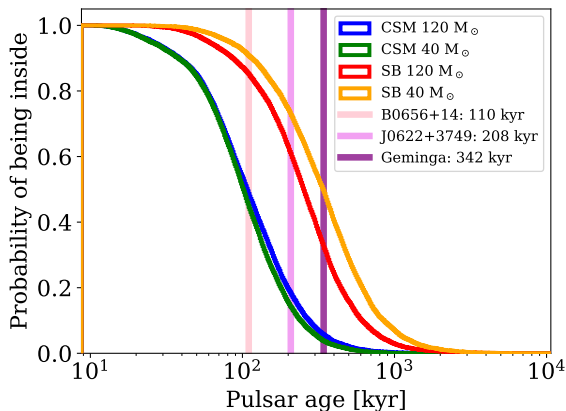


Figure: Probability of pulsars being inside the **bubble (SB)** as a function of time for the **CSM (SB)** models respectively.

Two curves are added by changing the maximum mass of massive stars that create pulsars from 120 M_⊙ to 40 M_⊙ following [Sukhbold et al. \(2016\)](#).

Comparing the probability of being inside the boundary

Special case: exiting the SNR inside the bubble

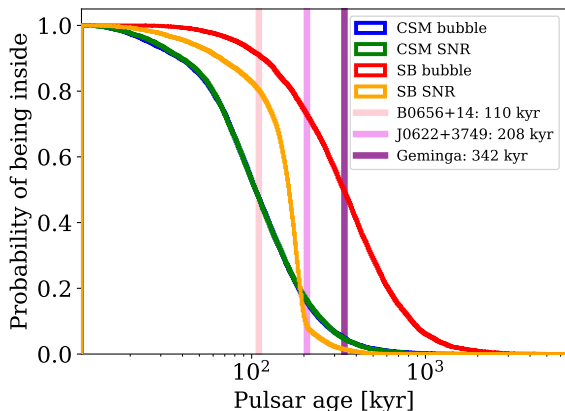


Figure: Probability of pulsars being inside the **bubble (SB)** as a function of time for the **CSM (SB)** models respectively. Max mass $40 M_{\odot}$. The **green** curve corresponds to the escape time of pulsars from the SNR inside the **CSM**, and the **orange** inside the **SB**.

Energy available for escaping pulsars

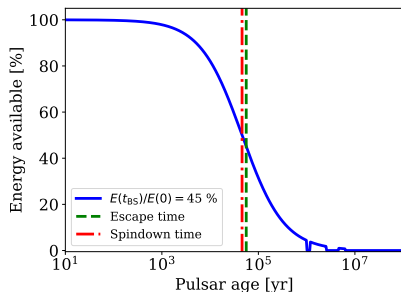


Figure: Evolution of the available energy of a pulsar as a function of time. Towards the later ages there are integration artifacts.

$P_0 = 100$ ms, $v_k = 280$ km/s as in [Evoli, Amato, et al. \(2021\)](#).

Energy available for escaping pulsars

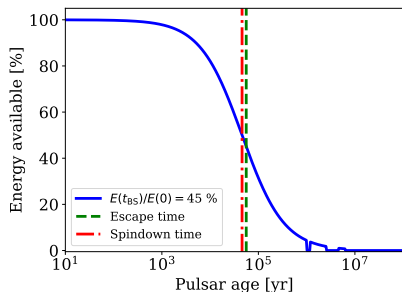


Figure: Evolution of the available energy of a pulsar as a function of time. Towards the later ages there are integration artifacts.

$P_0 = 100$ ms, $v_k = 280$ km/s as in [Evoli, Amato, et al. \(2021\)](#).

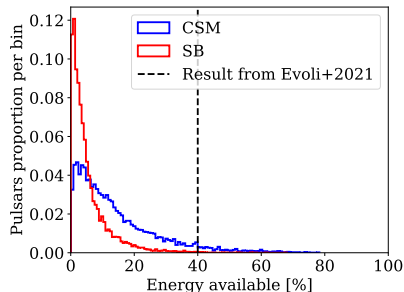


Figure: Distribution of available energies after escape. The initial period distribution comes from γ -ray observations in [Watters et al. \(2011\)](#).

Energy available for escaping pulsars

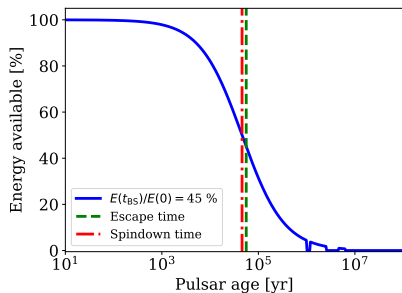


Figure: Evolution of the available energy of a pulsar as a function of time. Towards the later ages there are integration artifacts.

$P_0 = 100$ ms, $v_k = 280$ km/s as in [Evoli, Amato, et al. \(2021\)](#).

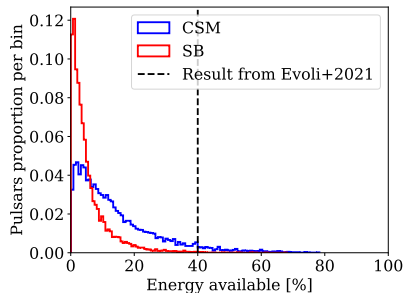


Figure: Distribution of available energies after escape. The initial period distribution comes from γ -ray observations in [Watters et al. \(2011\)](#).

Pulsars **DO NOT** have much energy left + leptons represent only a percentage of this energy

Summary

Main questions

Which medium are the leptons probing when we see a TeV halo?

Where is the pulsar at a given age?

Summary

Main questions

Which medium are the leptons probing when we see a TeV halo?
Where is the pulsar at a given age?

Conclusions

- Typically assumed: ~ 50 kyr and probe the ISM.
- We find instead a majority of $\gtrsim 100$ kyr pulsars are inside the **CSM/SB**.
- Are Geminga and PSR B0656+14 in a **hot and turbulent** environment?
- How are CSM/SB connected to **TeV halos**?
- How about similar pulsars in **radio**?

In the same project

- Add the **OB star association** as a possible model for the evolution of the system
- Create a **Galactic statistic** assuming probabilities of pulsars being born in one or another region

New projects: looking at the injection

- Investigate the contribution of **millisecond pulsars** to the CR lepton spectrum
- Work on the injection of leptons in the **interaction between the PWN and the SNR** using MHD simulations

Events attended

Conference

- **Talk in person at RICAP-2024** (Roma International Conference on Astro-Particle Physics), Roma Tre, Frascati

Workshop

- Participation in person to the **Workshop on Numerical Multi-Messenger Modelling** by Astroparticule et Cosmologie, Paris
- Participation in person to the **Conference in memory of Veniamin Berezinskii**, GSSI, L'Aquila

Summer School

- Participation in person to the **MPIK-CDY School on the Future of Gamma-Ray Astronomy** by the Max Planck Institute fur Kernphysik, Heidelberg

Bibliography I



Abeysekara, A. U. et al. (Nov. 2017). "Extended gamma-ray sources around pulsars constrain the origin of the positron flux at Earth". In: *Science* 358.6365, pp. 911–914. doi: 10.1126/science.aan4880. arXiv: 1711.06223 [astro-ph.HE].



Caraveo, P. A. et al. (Sept. 2003). "Geminga's Tails: A Pulsar Bow Shock Probing the Interstellar Medium". In: *Science* 301.5638, pp. 1345–1348. doi: 10.1126/science.1086973.



Cioffi, Denis F. et al. (Nov. 1988). "Dynamics of Radiative Supernova Remnants". In: *ApJ* 334, p. 252. doi: 10.1086/166834.



de Wit, W. J. et al. (July 2005). "The origin of massive O-type field stars: II. Field O stars as runaways". In: *A&A* 437.1, pp. 247–255. doi: 10.1051/0004-6361:20042489. arXiv: astro-ph/0503337 [astro-ph].



Evoli, Carmelo, Elena Amato, et al. (Apr. 2021). "Galactic factories of cosmic-ray electrons and positrons". In: *Phys. Rev. D* 103.8, 083010, p. 083010. doi: 10.1103/PhysRevD.103.083010. arXiv: 2010.11955 [astro-ph.HE].



Evoli, Carmelo, Tim Linden, et al. (Sept. 2018). "Self-generated cosmic-ray confinement in TeV halos: Implications for TeV γ -ray emission and the positron excess". In: *Phys. Rev. D* 98.6, 063017, p. 063017. doi: 10.1103/PhysRevD.98.063017. arXiv: 1807.09263 [astro-ph.HE].



Fang, Kun et al. (Sept. 2019). "Possible origin of the slow-diffusion region around Geminga". In: *MNRAS* 488.3, pp. 4074–4080. doi: 10.1093/mnras/stz1974. arXiv: 1903.06421 [astro-ph.HE].



Faucher-Giguère, Claude-André and Victoria M. Kaspi (May 2006). "Birth and Evolution of Isolated Radio Pulsars". In: *ApJ* 643.1, pp. 332–355. doi: 10.1086/501516. arXiv: astro-ph/0512585 [astro-ph].



Giacinti, G. et al. (Apr. 2020). "Halo fraction in TeV-bright pulsar wind nebulae". In: *A&A* 636, A113, A113. doi: 10.1051/0004-6361/201936505. arXiv: 1907.12121 [astro-ph.HE].

Bibliography II



Härer, Lucia K. et al. (Mar. 2023). "Understanding the TeV γ -ray emission surrounding the young massive star cluster Westerlund 1". In: *A&A* 671, A4, A4. doi: 10.1051/0004-6361/202245444. arXiv: 2301.10496 [astro-ph.HE].



Knies, Jonathan R. et al. (July 2018). "Suzaku observations of the Monogem Ring and the origin of the Gemini H α ring". In: *MNRAS* 477.4, pp. 4414–4422. doi: 10.1093/mnras/sty915.



Leahy, D. A., S. Ranasinghe, et al. (May 2020). "Evolutionary Models for 43 Galactic Supernova Remnants with Distances and X-Ray Spectra". In: *ApJS* 248.1, 16, p. 16. doi: 10.3847/1538-4365/ab8bd9. arXiv: 2003.08998 [astro-ph.HE].



Leahy, D. A. and J. E. Williams (May 2017). "A Python Calculator for Supernova Remnant Evolution". In: *AJ* 153.5, 239, p. 239. doi: 10.3847/1538-3881/aa6af6. arXiv: 1701.05942 [astro-ph.HE].



Mac Low, Mordecai-Mark and Richard McCray (Jan. 1988). "Superbubbles in Disk Galaxies". In: *ApJ* 324, p. 776. doi: 10.1086/165936.



Manchester, R. N. et al. (Apr. 2005). "The Australia Telescope National Facility Pulsar Catalogue". In: *AJ* 129.4, pp. 1993–2006. doi: 10.1086/428488. arXiv: astro-ph/0412641 [astro-ph].



Mukhopadhyay, Payel and Tim Linden (June 2022). "Self-generated cosmic-ray turbulence can explain the morphology of TeV halos". In: *Phys. Rev. D* 105.12, 123008, p. 123008. doi: 10.1103/PhysRevD.105.123008. arXiv: 2111.01143 [astro-ph.HE].



Parizot, E. et al. (Sept. 2004). "Superbubbles and energetic particles in the Galaxy. I. Collective effects of particle acceleration". In: *A&A* 424, pp. 747–760. doi: 10.1051/0004-6361:20041269. arXiv: astro-ph/0405531 [astro-ph].



Portegies Zwart, Simon F. et al. (Sept. 2010). "Young Massive Star Clusters". In: *ARA&A* 48, pp. 431–493. doi: 10.1146/annurev-astro-081309-130834. arXiv: 1002.1961 [astro-ph.GA].

Bibliography III



Schroer, B. et al. (May 2022). "Cosmic-ray generated bubbles around their sources". In: *MNRAS* 512.1, pp. 233–244. doi: 10.1093/mnras/stac466. arXiv: 2202.05814 [astro-ph.HE].



Seo, Jeongbhin et al. (Apr. 2018). "The Contribution of Stellar Winds to Cosmic Ray Production". In: *Journal of Korean Astronomical Society* 51.2, pp. 37–48. doi: 10.5303/JKAS.2018.51.2.37. arXiv: 1804.07486 [astro-ph.HE].



Sukhbold, Tuguldur et al. (Apr. 2016). "Core-collapse Supernovae from 9 to 120 Solar Masses Based on Neutrino-powered Explosions". In: *ApJ* 821.1, 38, p. 38. doi: 10.3847/0004-637X/821/1/38. arXiv: 1510.04643 [astro-ph.HE].



Watters, Kyle P. and Roger W. Romani (Feb. 2011). "The Galactic Population of Young gamma-ray Pulsars". In: *ApJ* 727.2, 123, p. 123. doi: 10.1088/0004-637X/727/2/123. arXiv: 1009.5305 [astro-ph.HE].



Weaver, R. et al. (Dec. 1977). "Interstellar bubbles. II. Structure and evolution.". In: *ApJ* 218, pp. 377–395. doi: 10.1086/155692.

CSM model

Theoretical framework for the SNR shock

Time (Numerically integrated)

$$t(R_s) = \int_0^{R_s} \frac{1}{u_s(r)} dr \quad (4)$$

Speed (Analytical)

$$u_s(R_s) = \frac{\gamma + 1}{2} \left[\frac{2\alpha E_{SN}}{M^2(R_s) R_s^\alpha} \times \int_0^{R_s} r^{\alpha-1} M(r) dr \right] \quad (5)$$

with $\alpha = 6(\gamma - 1)/(\gamma + 1)$.

Mass (Analytical)

$$M(r) = M_{ej} + 4\pi \int_0^r r'^2 \rho(r') dr' \quad (6)$$

CSM model

Density profile

The numbers (model from Weaver et al. (1977))

Wind region ($R_s < r_w$):

$$\rho_w(R_s) = \frac{\dot{M}}{4\pi u_w R_s^2}$$

Bubble region ($r_w < R_s < r_b$):

$$\rho_b(R_s) = \rho_b$$

Shell region ($r_b < R_s < r_{\text{ISM}}$):

$$\rho_{\text{shell}} = \frac{M_{\text{shell}}}{V_{\text{shell}}} = \frac{\frac{4\pi}{3} r_b^3 \rho_{\text{ISM}}}{\frac{4\pi}{3} (r_{\text{ISM}}^3 - r_b^3)}$$

ISM region ($r_{\text{ISM}} < R_s$):

$$\rho_{\text{ISM}} = 1 \text{ cm}^{-3}$$

CSM model

Looking at all the distributions

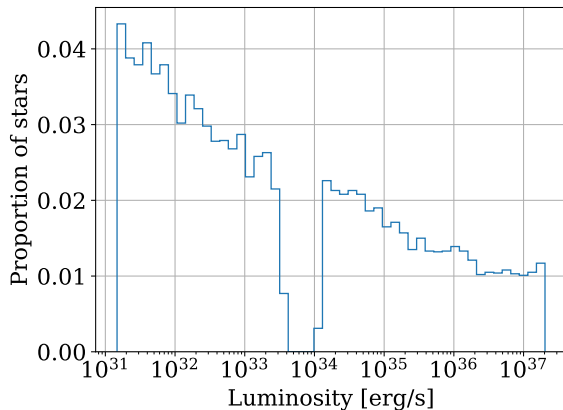


Figure: Luminosity distribution.

CSM model

Looking at all the distributions

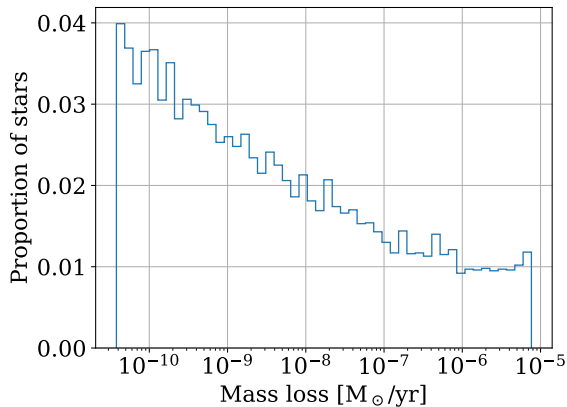


Figure: Mass loss distribution.

CSM model

Looking at all the distributions

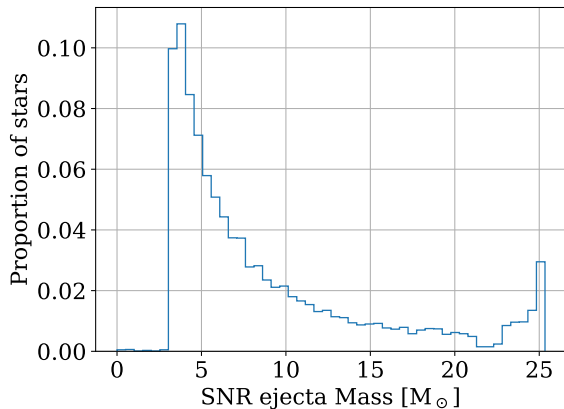


Figure: SNR ejecta mass distribution.

CSM model

Looking at all the distributions

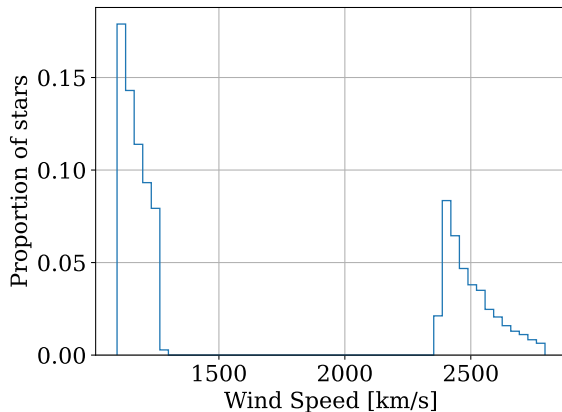


Figure: Wind speed distribution.

CSM model

Looking at all the distributions

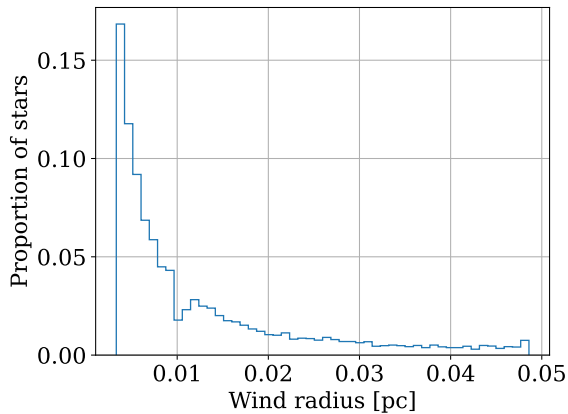


Figure: Wind radius distribution.

CSM model

Looking at all the distributions

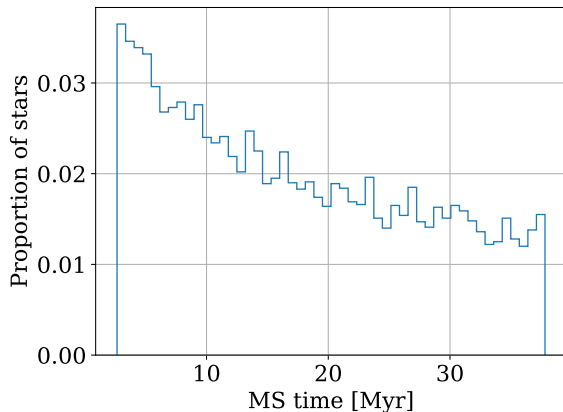


Figure: Main sequence time distribution.

CSM model

Looking at all the distributions

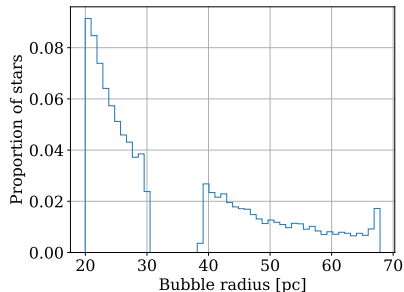


Figure: Bubble radius distribution.

Formula

From Weaver et al. (1977) and Härer et al. (2023):

$$r_b = 21 \text{ pc } \zeta_b^{1/5} L_{36}^{1/5} n_{\text{ISM},1}^{-1/5} t_6^{3/5} \quad (7)$$

CSM model

Looking at all the distributions

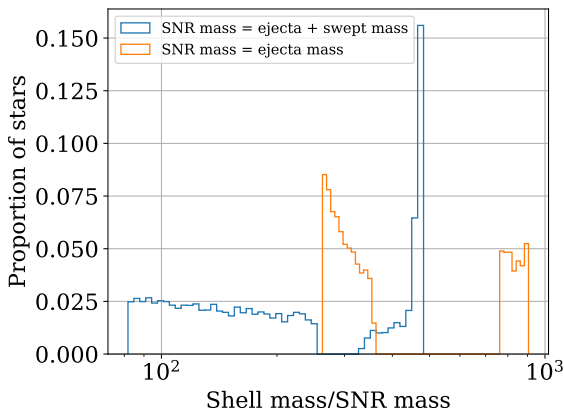


Figure: Shell mass/SNR mass distribution. We show for both the ejecta mass and the swept mass. Naturally, the swept mass is higher than the ejecta mass, resulting in a lower (by less than an order of magnitude) ratio. The shape in two parts of the orange curve is linked to the shape of the bubble radius (which is the determining factor for the parameter).

CSM model

Density profile

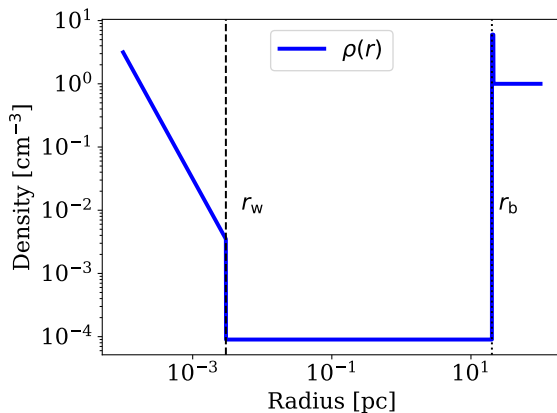


Figure: Density profile in the CSM, based on [Weaver et al. \(1977\)](#).

CSM model

Mass profile

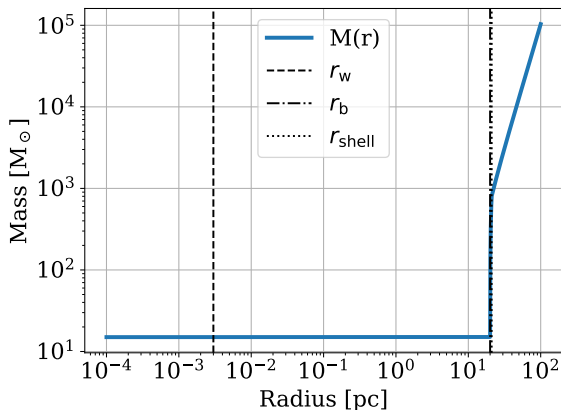


Figure: Accumulated mass profile in the CSM, analytically computed from the density profile

CSM model

Speed profile

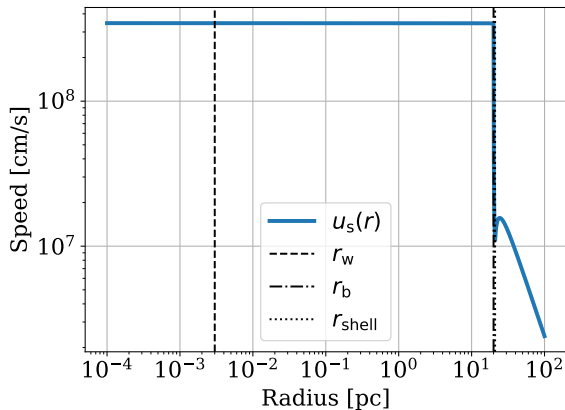


Figure: Accumulated speed profile in the CSM, analytically computed from the mass profile

Radiative phase

$$t_{\text{rad}} = \frac{3}{2} \frac{k_b T}{n \Lambda(T)}$$

with $\Lambda(T) = 1.6 \times 10^{-19} T^{-1/2}$ erg/cm³/s. We always go radiative when reaching the shell.

Merger with the bubble shell

$$u_s(R_s) = \beta c_{\text{sound}}(T(R_s))$$

with $\beta = 3$ and the speed of sound c_{sound} depending on the temperature profile found in [Weaver et al. \(1977\)](#). Since the SNR stops inside the shell, it merges there.

SB model

Looking at all the distributions

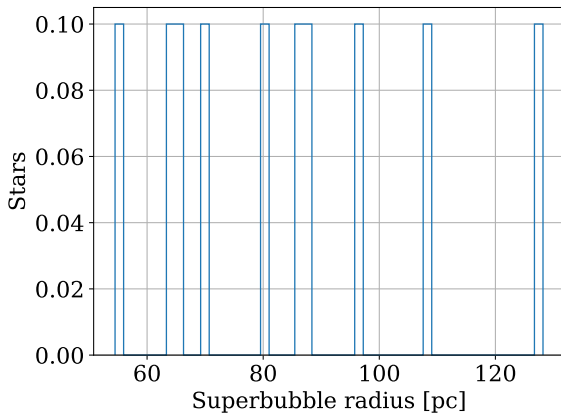


Figure: Superbubble radius distribution.